iScience

CellPress
OPEN ACCESS

Article

Electro-polarization of protein-like substances accelerates trans-cell-wall electron transfer in microbial extracellular respiration

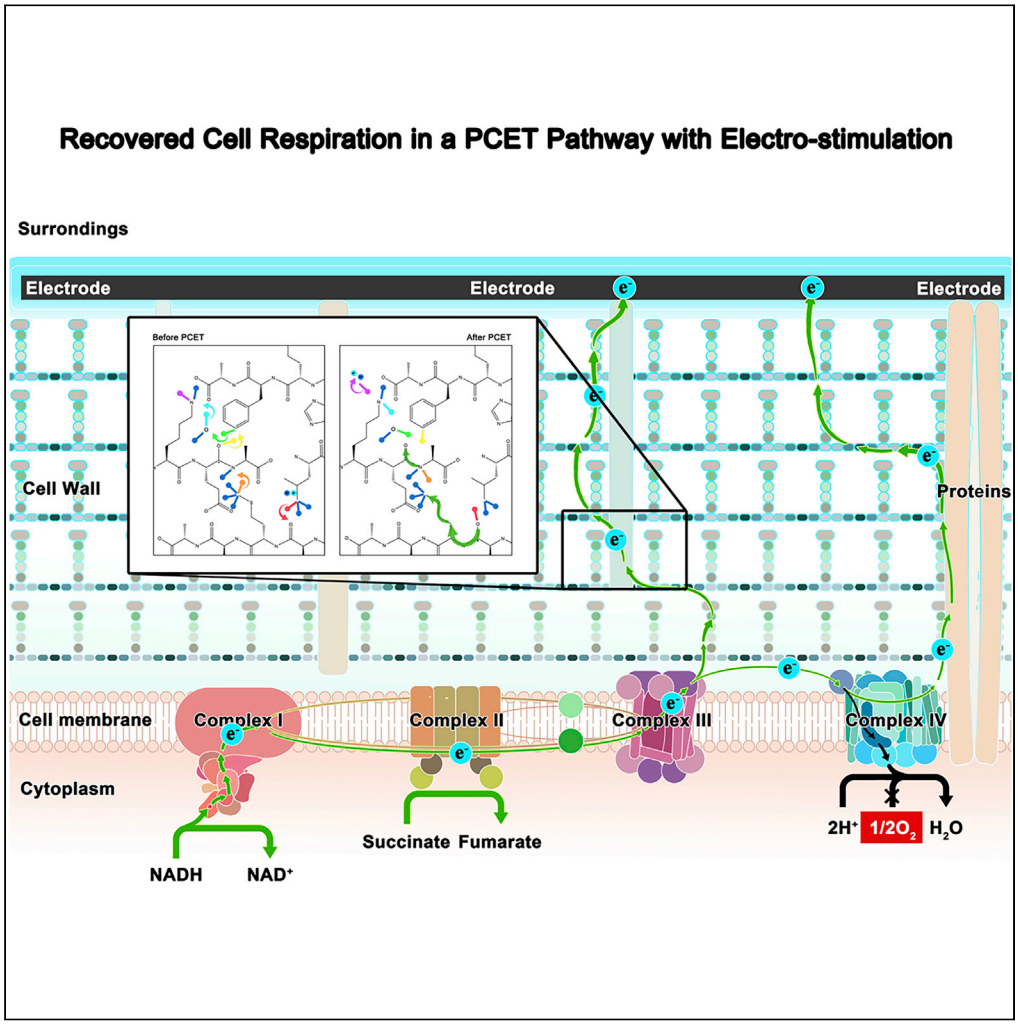

Qilin Yu, Haohao Mao, Bowen Yang, ..., Zhiqiang Zhao, Yang Li, Yaobin Zhang

zhangyb@dlut.edu.cn

Highlights

Inert proteins could be modified to enhance proton-coupled electron transfer

Protein-like substances in the cell wall could serve as electron relay sites

Trans-envelop electron transfer pathway could be established after modification

Common microbes could conduct extracellular respiration after domestication

Yu et al., iScience *26*, 106065
February 17, 2023
https://doi.org/10.1016/j.isci.2023.106065

iScience

CellPress
OPEN ACCESS

Article

Electro-polarization of protein-like substances accelerates trans-cell-wall electron transfer in microbial extracellular respiration

Qilin Yu,[1] Haohao Mao,[1] Bowen Yang,[1] Yahui Zhu,[1] Cheng Sun,[1] Zhiqiang Zhao,[1] Yang Li,[2] and Yaobin Zhang[1,3,*]

SUMMARY

Electrical stimulation has been used to strengthen microbial extracellular electron transfer (EET), however, the deep-seated reasons remain unclear. Here we reported that *Bacillus subtilis*, a typical gram-positive bacterium capable of extracellular respiration, obtained a higher EET capacity after the electrical domestication. After the electrical domestication, the current generated by the EET of *B. subtilis* was 23.4-fold that of the control group without pre-domestication. Multiple lines of evidence in bacterial cells of *B. subtilis*, their cell walls, and a model tripeptide indicated that the polarization of amide groups after the electrical stimulation forwarded the H-bonds recombination and radical generation of protein-like substances to develop extracellular electron transfer via the proton-coupled pattern. The improved electrochemical properties of protein-like substances benefited the *trans*-cell-wall electron transfer and strengthen extracellular respiration. This study was the first exploration to promote microbial extracellular respiration by improving the electrochemical properties of protein-like substances in cell envelopes.

INTRODUCTION

Microbial extracellular respiration, the core step of many important geochemical and biological processes such as dissimilatory iron reduction, bio-electrochemical systems (BESs), direct interspecies electron transfer, et al., has shown enormous potential in wastes treatment, pollution remediation, and biomass energy recovery.[1,2] Exoelectrogens develop multiple modules (such as E-pili and electron shuttle) to transport intracellular electrons through the cell wall and membrane to extracellular insoluble electron acceptors.[3,4] However, the thick cell wall mainly composed of electrically inert substances (such as peptidoglycan) limits the extracellular electron transfer.[5–7]

Electric potential stimulation has been found to strengthen extracellular electron transfer.[8,9] In BESs, the anodic oxidation of substrates is frequently enhanced with the increase of electricity generation over the operation, especially during the stage of domestication.[10,11] Many researchers attributed the enhancement of anodic oxidation to the enrichment of exoelectrogens since exoelectrogens can grow with the anode as the extracellular electron acceptor to produce the energy from substrate oxidation.[12,13] However, it was also found that some BESs could still perform well even with a low abundance of exoelectrogens. For example, in a study on the microbial electrolysis cell (MEC) for wastewater treatment,[14] the electric current of the MEC reactors increased with the decrease in the relative abundance of total exoelectrogens from 35.12% to 28.89%. Zakaria et al.[15] found that the current of the MEC was almost unchangeable when the relative abundance of exoelectrogens decreased significantly. Therefore, the enrichment of exoelectrogens was not the sole reason for the promotion of MECs performances.

Electro-activity of the microbial community has been regarded as the indicator to evaluate the EET of microbial aggregates.[16] The increase in the sludge electro-activity has been extensively reported in the EET-related processes including BESs,[17] direct interspecies electron transfer,[18] Feammox,[19] and so forth. The similarity of these systems is that the conductivity and capacitance of microbial aggregates were frequently found to increase with the operation. Generally, the improvement of the electro-activity was attributed to the changes in functional groups of cell/sludge or the decrease in internal resistances.[20] Until now, the deep reasons for the changes in electrochemical properties remain unclear.

[1]Key Laboratory of Industrial Ecology and Environmental Engineering (Dalian University of Technology), Ministry of Education, School of Environmental Science and Technology, Dalian University of Technology, Dalian 116024, China

[2]School of Ocean Science and Technology, Dalian University of Technology, Panjin, Liaoning 124221, China

[3]Lead contact

*Correspondence: zhangyb@dlut.edu.cn

https://doi.org/10.1016/j.isci.2023.106065

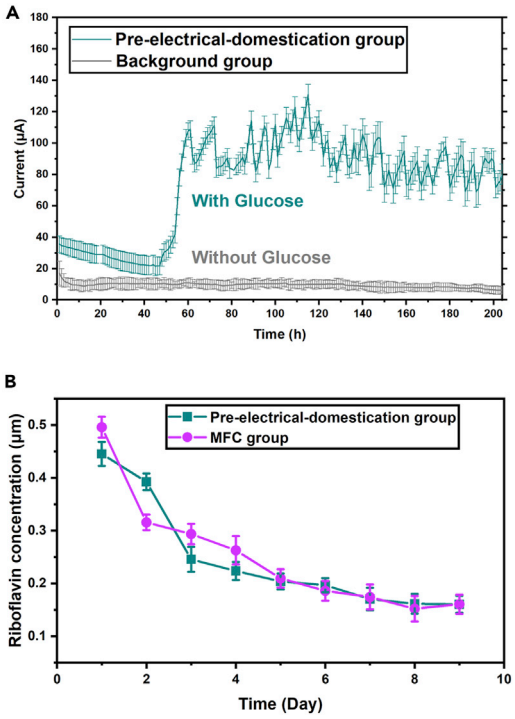

Figure 1. Operating performances of the reactors

(A) Current profiles along the pre-electrical domestication (green line vs gray line of a glucose-free MEC to show a background current)and (B) change profiles of riboflavin concentrations in the effluent of the pre-electrical-domestication group and MFC group (In this study, the error bars in all figures represent SD.).

Protein-like substances, such as peptidoglycans and membrane proteins composing amino acids or peptide chains,[21,22] are the essential components in cells and extracellular polymeric substances (EPS), which play vital roles in microbial respiration. Apart from the typical electro-active proteins (e.g., cytochrome *c* and Complex III),[23,24] amide groups in common protein-like substances also serve as the sites for electron transfer.[25] It was reported that applying electric potential induced the polarity of amide groups to promote the electron transfer of protein-like substances.[26] The polarization of C=O of amide groups and depolarization of the N−H groups in the sludge benefited the breaking and bonding of H-bonds to transport electrons via coupling with H motions.[27] Reasonably, we speculated that the cell wall mainly composed of protein-like substances were likely modified with electric potential, and it might improve the electro-activity of cells to enhance extracellular respiration. However, no studies have been reported on the effects of electrical stimulation on the electro-activity of cells in extracellular electron transfer.

In this study, *Bacillus subtilis*, a typical gram-positive bacterium with thick peptidoglycans that can conduct extracellular respiration under anaerobic conditions through secreting riboflavin as electron shuttle and also conduct aerobic respiration,[11,28] were domesticated with electrical stimulation to develop EET via enhancing the electro-activity of the cell walls. The changes in electron transfer of protein-like substances in cell walls were also explored.

RESULTS

Effects of electrical domestication on the electric current generation of *B. subtilis*

A MEC inoculated with *B. subtilis* in the anode (imposed with a potential of 0.3 V vs. Ag/AgCl) was operated. The continuous feeding mode was adopted to wash out the riboflavin secreted to exclude its role as an electron shuttle in the anode oxidation and the electric current production. In the initial 2 days, with the continuous feed, a tiny current between the anode and cathode of MEC likely related to the residual riboflavin slowly decreased to about 21.65 μA (Figure 1A), which was comparable to the background current of a glucose-free control MEC (no substrate as the anodic electron donor, i.e., no current generation). Afterward, the current drastically increased by about four times to a range of 81.04-112.52 μA. Meanwhile, the riboflavin concentration decreased from the initial 0.50 ± 0.02 mg/L (Day 1, Numbers those follow the ± sign are SD in this study, n = 3) to 0.16 ± 0.02 mg/L (Day 9, Figure 1B), indicating that the increase in the current was not due to the riboflavin. Considering that the electric current generation of

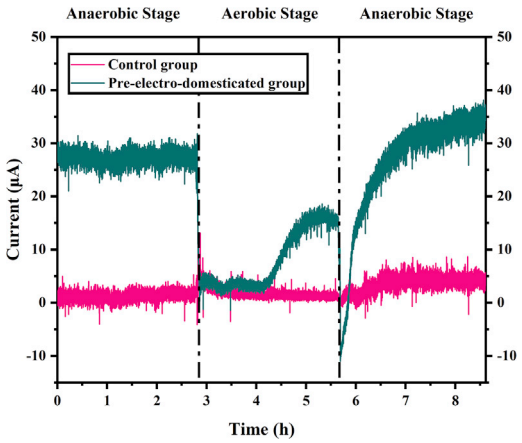

Figure 2. Electron acceptor switching test under the anaerobic-aerobic-anaerobic condition with the bacteria solution of pre-electrical-domestication group and aerobic control group

MEC is a result of the electron transfer from bacteria to the anode, it is reasonable to assume that the electrical domestication was likely the reason for the enhancing EET of the bacteria.

The *B. subtilis* after the pre-electrical domestication was partly inoculated into a new MEC to conduct a short-term electron acceptor switching test under anaerobic-aerobic-anaerobic conditions to further investigate the effects of electrical domestication. As a control test, another group of *B. subtilis* that had been aerobically cultured for 9 days in advance was parallelly operated under the same conditions (including the same cell concentration and viability). In the initial anaerobic stage (0-2.81 h), the current generation of the pre-electrical-domestication group was maintained at 26.91 $\pm$ 0.83 μA, which was 23.4 times that of the control group that was pre-aerobic operated without electrical domestication ahead (1.15 $\pm$ 0.61 μA, 0-1 h) (Figure 2). The higher current generation of the pre-electrically domestication indicated that the EET of *B. subtilis* was significantly promoted after the electrical domestication.

When shifting the anaerobic condition (i.e., N_2/CO_2 aeration) to O_2 aeration (Figure 2), the current of the pre-electrical-domestication group sharply decreased from 26.91 $\pm$ 0.83 to 3.18 $\pm$ 0.45 μA (2.81-3.81 h) which approached to the control group (i.e., aerobically cultured without electrical domestication), indicating that *B. subtilis* preferred to use oxygen as the terminal electron acceptor. Then, the current raised to about 17.07 μA, due to the unstable oxygen aeration. When turning to the anaerobic condition again, the current raised rapidly to 34.81 $\pm$ 1.26 μA (7.61-8.61 h) following a reverse current resulting from the shifting aeration operation. Comparatively, the electric current of the control group was maintained at a low level during the entire test. Although the control group was also shifted to the anaerobic condition with the electrical stimulation, the short hours of electrical stimulation were not enough for the bacteria of control to develop the ability of EET besides secreting the electron shuttle (i.e., riboflavin), which was consistent with the slight current in the initial two days of electrical domestication (Figure 1A). Moreover, such phenomenon still occurred in more cycles (Figure S1A). It meant that when shifting back to the anaerobic condition, *B. subtilis* after the pre-electrical domestication recovered the extracellular respiration to generate the current. With switching the electron acceptor between the anode (i.e., anaerobic condition) and oxygen, the significant current change was a result of the shifting of respiration mode between extracellular respiration and intracellular respiration.

It has been well known that *B. subtilis* is a facultative anaerobic bacterium that capable of secreting riboflavin as electron shuttles to conduct extracellular respiration under anaerobic conditions,[29–31] but this is the first time to find this kind of bacteria could develop the extracellular respiration through the electric domestication with a decreasing riboflavin concentration.

The genomic responses to oxygen (aerobic) and electricity (anaerobic) were also a factor that may affect microbial respiration such as the secretion of respiration complexes and riboflavin. However, the concentrations of Complex I and Complex III in the pre-electrical-domestication group and control group were similar, and that of the control group was even slightly higher than that of the pre-electrical-domestication group (Figure S1B). Therefore, the increased current was not due to the secretion of respiratory enzymes.

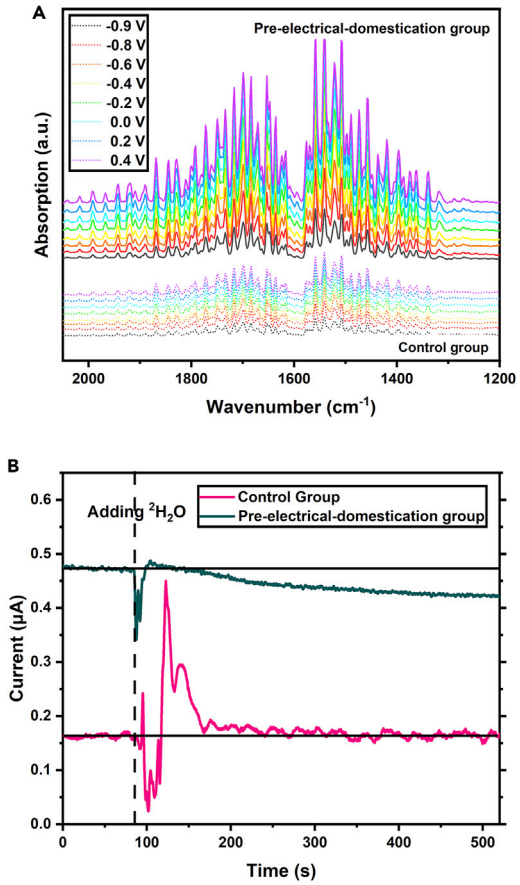

Figure 3. Changes in the electon transfer pattern of *B. subtilis*

(A) Electrochemical *in situ* FTIR spectra of pre-electrical-domestication group (solid line) and control group (dotted line) and (B) chronoamperometry results of the pre-electrical-domestication group and control group after $^{2}H_2O$ was added to the substrate.

Polarization of functional groups of *B. subtilis* after the electrical domestication to develop extracellular electron transfer

The bacteria cells collected from the pre-electrical-domestication group and control group after the anaerobic-aerobic-anaerobic shifting test were identified by electrochemical *in situ* Fourier transform infrared spectroscopy (FTIR) to observe the possible changes of functional groups of the cell surface to gradient potentials at the molecular level. As shown in Figure 3A, the intensities of C–N (bands around 1550 cm^{-1}) and C=O bands (bands around 1650 cm^{-1}) in amide groups[27] of aerobic-cultured bacteria (control group) had fewer changes and were lower than that of the pre-electrical-domestication group, indicating that the amide groups of aerobic-cultured bacteria were inert to the electric signals. Comparatively, for the bacteria of the pre-electrical-domestication group, the intensities of C–N and C=O bands in amide groups increased significantly with the potential shifting from −0.9 V to 0.4 V, which was the result of the polarization of C–N and C=O in amide groups.[32,33] The polarity was reported to be positively related to the relative permittivity that indicated the capacitance of the material.[34] Therefore, the polarization of amide groups with the potential could increase the capacitance of amide groups on the cell surface.

After the pre-electrical-domestication, the polarization of amide groups (i.e., C–N and C=O) led to the electrons around N and O atoms getting into higher energy states. In this way, these electrons may participate in electron transfer (see the Kelvin probe force microscopy test later in discussion). Meanwhile, C–N and C=O in amide groups were reported to be essential sites for the electron transfer in protein-like substances.[35] Specifically, C=O could accept protons or H radicals to form •C–O–H to transport electrons, termed proton-coupled electron transfer.[36] The polarized amide groups of cell surface meant that more

electrons in higher energy states could participate in the extracellular respiration via the proton-coupled pattern.

To confirm the proton-coupled electron transfer, a $^{2}H/^{1}H$ kinetic isotope effect (KIE) test was conducted to further investigate the EET of *B. subtilis*.[37] As shown in Figure 3B, the initial current of the pre-electrical-domestication group was higher (1.93-fold) than that of the control group before the addition of deuterated water ($^{2}H_2O$), indicating a higher conductivity of the bacteria after the pre-electrical domestication. Noteworthily, the initial current of control was a result of instinctive EET with its secretion as the electron shuttle under the batch mode of the KIE test. After the addition of deuterated water ($^{2}H_2O$), the current of the pre-electrical-domestication group showed a continuous decrease and eventually maintained at a lower level than that before adding $^{2}H_2O$, while the current of the control group recovered to the same level as the initial after fluctuations. With the addition of $^{2}H_2O$, the ^{2}H with higher mass replaced ^{1}H (proton) of $^{1}H_2O$ to inevitably slow down the proton motion and electron transfer resulting in the current decrease. It indicated that the development of ^{1}H-coupled electron transfer after the electrical domestication was the main reason for the increased current generation and EET of *B. subtilis* in this study. Together with the polarized amide groups of the cell surface in FTIR results, it seemed that the protein-like substances of the cell walls were modified to enhance *trans*-cell-wall electron transfer.

Electro-activity of the cell walls of *B. subtilis* after the electrical treatment

Cell walls of the original *B. subtilis* were extracted (Figure S2) and then polarized for 10 days by a potentiostat (0.3 V vs. Ag/AgCl) to further verify the effects of potential treatment (referred to as the potential-treated group). The conductivity of (Figure S3A) the cell walls of the potential-treated group (486.67 $\pm$ 5.77 μS/cm, n = 3) was 3.42-folder higher than that of the potential-free group (parallel with the potential group but not polarized, 141.90 $\pm$ 3.99 μS/cm, n = 3), in agreement with the current generation Figures 1A and 2. The current of the cell wall solution of the potential-treated group also showed a continuously decreased current after the addition of $^{2}H_2O$, which was a significant $^{2}H/^{1}H$ kinetic isotope effect (Figure S3B). While little changes in the current were observed in the cell walls solution prepared by the control group. It further indicated that ^{1}H-coupled electron transfer occurred in the current generation of cell walls after the electrical treatment (Figure 3B).

From the Kelvin probe force microscopy (KPFM) spectra of the extracted cell walls (light spots in the red circle in Figures 4A and 4B), a discrepancy in the surface potential (Figures 4C and 4D) was observed between the cell walls of the potential-free group and the potential-treated group. For the cell walls of the potential-treated group, the surface potential profile along the hatching line showed two crests across the cell walls (Figure 4F). The corresponding surface potential was much higher (by 55.9 mV) than that of the backing material (nonconducting glass). While for the cell walls of the potential-free group, the surface potential profile there were no crest and fewer changes (in a range of 33.8 mV) of the surface potential across the cell walls along with the hatching line (Figure 4E). The higher surface potential of the potential-treated cell walls meant that the electron of the cell walls was at a higher Fermi level (lower escaping power) to be more likely excited to the conduction band to participate in the electron transfer of the cell walls and produce the electric current.[38–40]

Reconfirmation of improved electro-activity of a model tripeptide with the electrical stimulation

To further investigate the reason for the conductivity changes of the cell walls and the roles of protein-like substances in the enhanced EET,[41,42] a model tripeptide, Leu tripeptide (L-Leu-L-Leu-L-Leu, Figure S4A) mainly composed of H-bond (including C—H and N—H) with no typical redox centers (such as porphyrin and [Fe-S] cluster), was used as the electrically inert peptide to investigate the possible changes of protein-like substances with the potential treatment.

Along with the potential stimulation for 10 days, the current of Leu tripeptide solution increased by 4.6-folds from 2.40 $\pm$ 0.28 μA (1-24 h) to 11.1 $\pm$ 0.43 μA (217-240 h) (after the background correction, Figure S4A). The increased current was a direct proof of improvement in the conductivity of the tripeptide, which was consistent with the increased conductivities of the cell walls (Figure S3A). Moreover, the capacitances of the potential-treated peptide solution were 2.29-fold higher than that of the potential-free group of electrically inert peptides (Figure S4B), indicating the improvement of electron storage capacity of the potential-treated tripeptide.

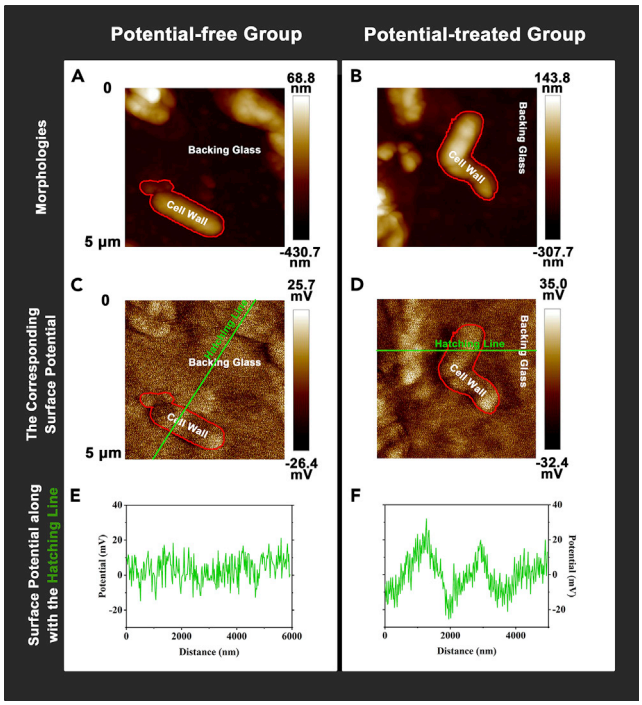

Figure 4. Morphologies (A, B), the corresponding surface potential (C, D), and potential profiles (E, F) of the cell walls in the potential-free group and the potential-treated group

Like most of electrically inert membrane proteins, Leu tripeptide has no typical redox centers to support electron tunneling. The only possible way for Leu tripeptide to transport electrons was to couple with the proton motion between H-bonds in peptide backbones and sidechains. The generation of C-centered radicals (like •C−O−H) was accompanied by the proton-coupled electron transfer in amide groups. The electron paramagnetic resonance (EPR) tests were conducted to investigate the radical generation of the tripeptide with the potential (electrolysis for 1 h). The EPR spectrum of the electro-treated group showed a dominant broad singlet (g = 2.0056) that was the superposition of N-centered (g = 2.0053-2.0059)[43] and/or C-centered (g = 2.0057)[44] radicals (Figure 5A), while no significant radical signal in the potential-free peptide. The results confirmed that the C-centered and/or N-centered radicals (like •C−O−H) were generated by the potential stimulation, further forwarding the proton-coupled electron transfer in protein-like substances.

From the X-ray photoelectron spectroscopy (XPS) spectra (Figure 5B), after the electric potential treatment, the binding energy of N 1s peak increased from 399.81 to 399.85 eV. In XPS spectra, the binding energy reflects the degree of difficulty for surface electrons to escape from the atoms. A higher binding energy of N atoms means that it is harder for the electrons on the surface of N atoms to escape. According to the electron configuration, the electrons of the outermost shell possess the lowest binding energy to escape from the N atoms. And the excursion of the outermost electrons from N atoms led to the exposure of inner electrons that were in higher binding energy. Therefore, the increased binding energy of N atoms implied that the outermost electrons on the N atom surface shifted to other atoms (such as the H atom in N−H groups).[45] The excursion of an electron from N atoms to H atoms led to the depolarization of the N−H bond to facilitate the hemolysis of N−H to product •H and then participate in proton-coupled electron transfer. Meanwhile, the decrease (from 531.76 to 531.28 eV) of the binding energy of O 1s peak after the potential treatment meant that the surface electrons of O atoms could be excited easily (Figure 5C). In Leu tripeptide, C is the main atom bonded with the O atom, and the decrease of the binding energy of O 1s indicated that more electrons moved from C to O atoms to polarize C=O, which was consistent with the FTIR results (Figure 3A).

The changes in the binding energy of N 1s and O 1s showed that the electrochemical properties of the functional groups were affected by the electrical treatment, which was also the reason for the polarization of amide groups. With the changes of amide groups (including polarization), the recombination of

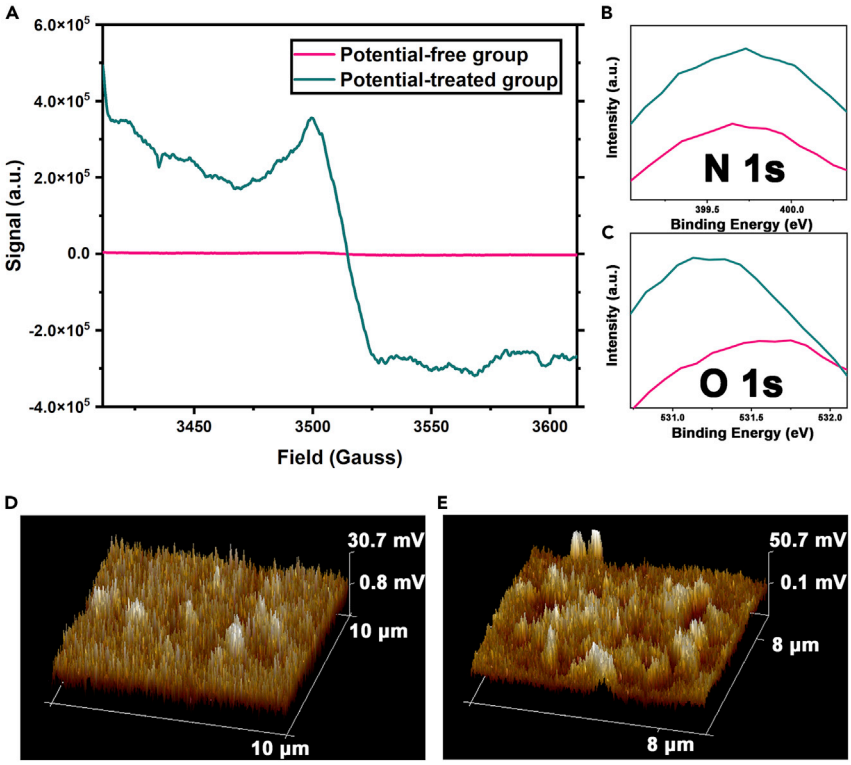

Figure 5. Effects of potential treatment on peptide nature

(A) electron paramagnetic resonance (EPR) results; (B) N 1s and (C) O 1s spectra of X-ray photoelectron spectroscopy (XPS) of the Leu-tripeptide in the potential-treated group and potential-free group; and Kelvin Probe Force Microscopy (KPFM) of the Leu-tripeptide in the potential-free group (D) and potential-treated group (E).

H-bonds as well as the radical generation occurred to forward the proton-coupled electron transfer in Leu tripeptide.

The KPFM test also showed that the potential-treated peptide had a higher surface potential (0.1-50.7 mV, 50.6 mV) than that of the potential-free peptide (0.8-30.7 mV, 29.9 mV) (Figures 5D and 5E). The higher surface potential of the potential-treated group meant that the electron in the peptide was at a higher Fermi level (lower escaping power), which was beneficial for the electron transfer in the tripeptide.

DISCUSSION

Conductive-pili, electron shuttles, and *C*-type cytochromes are the main electron transfer pathways for exoelectrogens to transport intercellular electrons through cell envelopes to extracellular electron acceptors.[46] Plenty of studies on BES systems showed that microbial extracellular respiration was gradually enhanced during the operation, frequently accompanied by the increase of the electro-activities of anaerobic aggregates. Commonly, the thick cell envelops mainly composed of electro-inner peptidoglycan were not considered to participate in EET.

After the electrical domestication, the current generated by *B. subtilis* was 23.4 times that of the background electric current caused by the few remaining electron shuttles secreted by bacteria. Multiple lines of evidence confirmed that the electrochemical properties of amide groups in protein-like substances were improved with electrical stimulation. Notably, the excursion of the electron from N to H or from C to O in amino acids induced the polarization of amide groups to forward the proton-coupled electron transfer in cell walls to develop extracellular respiration (Figure 6).

Microbes capable of extracellular respiration play an important role in nature and artificial biological treatment systems. However, the low efficiency of some biological treatment systems has been taken for

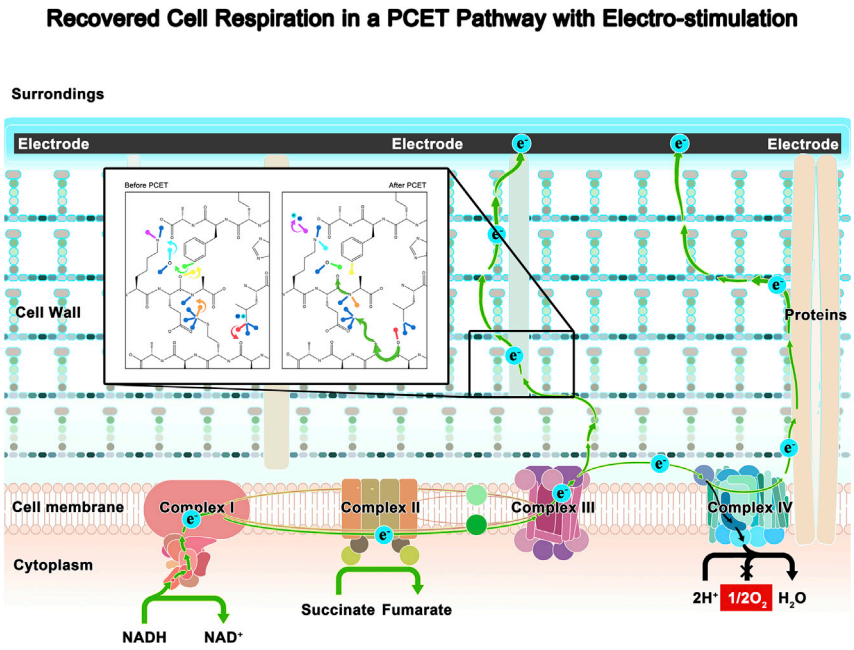

Figure 6. Schematic illustration of the *trans*-cell-wall electron transfer pathway assisted by proton-coupled electron transfer (PCET) for *B. subtilis* to achieve efficient extracellular electron transfer

granted due to the limitation of the traditional understanding. That is, the low efficiency of microbial processes related to extracellular respiration is commonly attributed to the failure to enrich electro-active bacteria. In this study, we found that after a period of electric potential treatment, the *trans*-cell-wall electron transfer could proceed within the electrically inert protein-like substances via the proton-coupled pattern. Using protein-like substances in cell walls as the electron carriers provide a new point of view to reinforce extracellular electron transfer, which is significantly important in some biological systems related to extracellular respiration, such as environmental remediation and biomass energy recovery. These results explained the reason for the improved electro-activity of microbial aggregations in BESs, that is, the electrical treatment induced the polarization of amide groups to promote the electron transfer along with protein-like substances in microbial aggregations. It is the first time to interpret that the electro-activities of electrically inert protein-like substances could be improved by electrical stimulation to be engaged in EET.

The bacteria (*B. subtilis*) used in this study was capable of secreting riboflavin to conduct the electron shuttle-dependent extracellular electron transfer. However, other types of microorganisms (even the extracellularly respiratory microorganism) may also obtain the improved EET capacity after electrical stimulation, for the tests of cell wall and model tripeptide all showed that the protein-like substance could be polarized to forward the proton-coupled electron transfer. Such effects of electrical stimulation on protein-like substances may be of universal significance, and more model-type microorganisms (e.g., *actinomyces* and *cyanobacteria*) with different cell wall characters will be investigated in future works to further investigate the effects of electrical stimulation on cell respiration.

In this study, *B. subtilis*, using electron shuttles to perform extracellular respiration, were electrically domesticated to investigate the effect of electrical stimulation on the *trans*-cell-wall electron transfer. With a decreasing concentration of electron shuttles, the *B. subtilis* still generated an increasing electric current. The conductivity of the cell walls also increased, showing the promoted electron transfer in the cell walls. Furtherly, the results in bacteria cells, cell walls, and the model tripeptide all indicated that the polarization of amide groups after the electrical stimulation forwarded the proton-coupled electron transfer along with protein-like substances to maintain extracellular respiration. This study explained the effects of electrical stimulation on microbial extracellular respiration from the chemical perspective, which was also the first exploration to promote microbial extracellular respiration by improving the electrochemical properties of protein-like substances in cell envelopes.

Limits of study

One limitation of this study is that it revealed the phenomenon that protein-like substances could be polarized with the anode potential, however, the possible reasons for the electrically induced changes in polarity of amide groups were not clearly illustrated. The applied potential may change the structure of protein-like substances to improve their electrical properties. Actually, it is an important issue to be addressed in our follow-up studies. Meanwhile, such effects of electrical stimulation on protein-like substances may be a universal phenomenon, which need to be confirmed with more species of microorganisms. Altogether, this study still revealed a significant phenomenon in bioelectrochemistry that has been long-termly ignored.

STAR★METHODS

Detailed methods are provided in the online version of this paper and include the following:

- KEY RESOURCES TABLE
- RESOURCE AVAILABILITY
  - Lead contact
  - Materials availability
  - Data and code availability
- EXPERIMENTAL MODEL AND SUBJECT DETAILS
  - *B. subtilis* strains and LEU Tri-peptide
- METHOD DETAILS
  - Extraction of cell walls
  - Bio-electro-chemical system (BES) setup
  - Electron acceptor switching test
  - Cell walls and tripeptide treatment batches
  - Detection of riboflavins
  - Detection of respiratory enzymes
  - Optical detection
  - Electrochemical measurements
  - *In situ* electrochemical test
  - Kinetic isotope effect (KIE) test
  - Atomic force microscope (AFM) test
  - Electron paramagnetic resonance spectroscopy
  - X-Ray photoelectron spectroscopy (XPS)
- QUANTIFICATION AND STATISTICAL ANALYSIS

SUPPLEMENTAL INFORMATION

Supplemental information can be found online at https://doi.org/10.1016/j.isci.2023.106065.

ACKNOWLEDGMENTS

The authors acknowledge the financial support from the National Natural Science Foundation of China (22276024, 51978122), State Key Research & Development Plan (2021YFA1201703), and Liaoning Revitalization Talents Program (XLYC1902075).

AUTHOR CONTRIBUTIONS

Y.Z. and Q.Y. conceived the study. Q.Y., H.M., and B.Y. carried out the experiments, Q.Y., Y.Z., and S.C. analyzed the experimental data. Y.Z. and Q.Y. wrote the article. Q.Y., Z.Z., and Y.L. discussed the results of the article.

DECLARATION OF INTERESTS

The authors declare no competing interests.

Received: August 25, 2022
Revised: December 22, 2022
Accepted: January 20, 2023
Published: February 01, 2023

REFERENCES

1. Richter, K., Schicklberger, M., and Gescher, J. (2012). Dissimilatory reduction of extracellular electron acceptors in anaerobic respiration. Appl. Environ. Microbiol. *78*, 913–921. https://doi.org/10.1128/AEM.06803-11.

2. Kato, S. (2015). Biotechnological aspects of microbial extracellular electron transfer. Microb. Environ. *30*, 133–139. https://doi.org/10.1264/jsme2.ME15028.

3. Unden, G., and Klein, R. (2021). Sensing of O2 and nitrate by bacteria: alternative strategies for transcriptional regulation of nitrate respiration by O2 and nitrate. Environ. Microbiol. *23*, 5–14. https://doi.org/10.1111/1462-2920.15293.

4. Wing, B.A., and Halevy, I. (2014). Intracellular metabolite levels shape sulfur isotope fractionation during microbial sulfate respiration. Proc. Natl. Acad. Sci. USA *111*, 18116–18125. https://doi.org/10.1073/pnas.1407502111.

5. White, G.F., Edwards, M.J., Gomez-Perez, L., Richardson, D.J., Butt, J.N., and Clarke, T.A. (2016). Mechanisms of bacterial extracellular electron exchange. Adv. Microb. Physiol. *68*, 87–138. https://doi.org/10.1016/bs.ampbs.2016.02.002.

6. Ma, C., Zhou, S., Zhuang, L., and Wu, C. (2011). Electron transfer mechanism of extracellular respiration: a review. Acta Ecol. Sin. *31*, 2008–2018.

7. Giese, B., Eckhardt, S., and Lauz, M. (2012). Electron Transfer in Peptides and Proteins (Encyclopedia of Radicals in Chemistry, Biology and Materials).

8. Kumar, S.S., Kumar, V., Malyan, S.K., Sharma, J., Mathimani, T., Maskarenj, M.S., Ghosh, P.C., and Pugazhendhi, A. (2019). Microbial fuel cells (MFCs) for bioelectrochemical treatment of different wastewater streams. Fuel *254*, 115526. https://doi.org/10.1016/j.fuel.2019.05.109.

9. Kumar, R., Singh, L., Wahid, Z.A., and Din, M.F.M. (2015). Exoelectrogens in microbial fuel cells toward bioelectricity generation: a review. Int. J. Energy Res. *39*, 1048–1067. https://doi.org/10.1002/er.3305.

10. Light, S.H., Su, L., Rivera-Lugo, R., Cornejo, J.A., Louie, A., Iavarone, A.T., Ajo-Franklin, C.M., and Portnoy, D.A. (2018). A flavin-based extracellular electron transfer mechanism in diverse Gram-positive bacteria. Nature *562*, 140–144. https://doi.org/10.1038/s41586-018-0498-z.

11. Nimje, V.R., Chen, C.Y., Chen, C.C., Jean, J.S., Reddy, A.S., Fan, C.W., Pan, K.Y., Liu, H.T., and Chen, J.L. (2009). Stable and high energy generation by a strain of Bacillus subtilis in a microbial fuel cell. J. Power Sources *190*, 258–263.

12. Lin, C., Wu, P., Liu, Y., Wong, J.W., Yong, X., Wu, X., Xie, X., Jia, H., and Zhou, J. (2019). Enhanced biogas production and biodegradation of phenanthrene in wastewater sludge treated anaerobic digestion reactors fitted with a bioelectrode system. Chem. Eng. J. *365*, 1–9. https://doi.org/10.1016/j.cej.2019.02.027.

13. Zhao, Z., Zhang, Y., Ma, W., Sun, J., Sun, S., and Quan, X. (2016). Enriching functional microbes with electrode to accelerate the decomposition of complex substrates during anaerobic digestion of municipal sludge. Biochem. Eng. J. *111*, 1–9. https://doi.org/10.1016/j.bej.2016.03.002.

14. Wang, B., Liu, W., Zhang, Y., and Wang, A. (2020). Intermittent electro field regulated mutualistic interspecies electron transfer away from the electrodes for bioenergy recovery from wastewater. Water Res. *185*, 116238. https://doi.org/10.1016/j.watres.2020.116238.

15. Zakaria, B.S., and Ranjan Dhar, B. (2021). An intermittent power supply scheme to minimize electrical energy input in a microbial electrolysis cell assisted anaerobic digester. Bioresour. Technol. *319*, 124109. https://doi.org/10.1016/j.biortech.2020.124109.

16. Li, C., Lesnik, K.L., and Liu, H. (2017). Stay connected: electrical conductivity of microbial aggregates. Biotechnol. Adv. *35*, 669–680. https://doi.org/10.1016/j.biotechadv.2017.07.010.

17. Madondo, N.I., Tetteh, E.K., Rathilal, S., and Bakare, B.F. (2021). Synergistic effect of magnetite and bioelectrochemical systems on anaerobic digestion. Bioengineering *8*, 198. https://doi.org/10.3390/bioengineering8120198.

18. Lovley, D.R. (2011). Reach out and touch someone: potential impact of DIET (direct interspecies energy transfer) on anaerobic biogeochemistry, bioremediation, and bioenergy. Rev. Environ. Sci. Biotechnol. *10*, 101–105. https://doi.org/10.1007/s11157-011-9236-9.

19. Guan, Q., Zhang, Y., Tao, Y., Chang, C.T., and Cao, W. (2019). Graphene functions as a conductive bridge to promote anaerobic ammonium oxidation coupled with iron reduction in mangrove sediment slurries. Geoderma *352*, 181–184. https://doi.org/10.1016/j.geoderma.2019.05.044.

20. Wang, B., Liu, W., Zhang, Y., and Wang, A. (2020). Bioenergy recovery from wastewater accelerated by solar power: intermittent electro-driving regulation and capacitive storage in biomass. Water Res. *175*, 115696. https://doi.org/10.1016/j.watres.2020.115696.

21. Gong, B., Du, M., Qian, C., Chen, W., Sit, P.H.L., Liu, X.W., and Yu, H.Q. (2021). Why should tryptones rather than bovine serum albumin Be used as model proteins to explore the interactions between proteins and pollutants in environments? Environ. Sci. Technol. Lett. *8*, 1038–1044.

22. Bourven, I., Costa, G., and Guibaud, G. (2012). Qualitative characterization of the protein fraction of exopolymeric substances (EPS) extracted with EDTA from sludge. Bioresour. Technol. *104*, 486–496. https://doi.org/10.1016/j.biortech.2011.11.033.

23. Camilo, S.R.G., Curtolo, F., Galassi, V.V., and Arantes, G.M.; Modeling (2021). Tunneling and nonadiabatic effects on a proton-coupled electron transfer model for the Q o site in cytochrome bc 1. J. Chem. Inf. Model. *61*, 1840–1849. https://doi.org/10.1021/acs.jcim.1c00008.

24. Saura, P., and Kaila, V.R.I. (2019). Energetics and dynamics of proton-coupled electron transfer in the NADH/FMN site of respiratory complex I. J. Am. Chem. Soc. *141*, 5710–5719. https://doi.org/10.1021/jacs.8b11059.

25. Chen, L., Li, X., Xie, Y., Liu, N., Qin, X., Chen, X., and Bu, Y. (2022). Modulation of proton-coupled electron transfer reactions in lysine-containing alpha-helixes: alpha-helixes promoting long-range electron transfer. Phys. Chem. Chem. Phys. *24*, 14592–14602. https://doi.org/10.1039/d2cp00666a.

26. Liu, X., Zhan, J., Liu, L., Gan, F., Ye, J., Nealson, K.H., Rensing, C., and Zhou, S. (2021). In situ spectroelectrochemical characterization reveals cytochrome-mediated electric syntrophy in geobacter coculture. Environ. Sci. Technol. *55*, 10142–10151. https://doi.org/10.1021/acs.est.1c00356.

27. Yu, Q., and Zhang, Y. (2019). Fouling-resistant biofilter of an anaerobic electrochemical membrane reactor. Nat. Commun. *10*, 4860. https://doi.org/10.1038/s41467-019-12838-7.

28. Gu, Y., Xu, X., Wu, Y., Niu, T., Liu, Y., Li, J., Du, G., and Liu, L. (2018). Advances and prospects of Bacillus subtilis cellular factories: from rational design to industrial applications. Metab. Eng. *50*, 109–121. https://doi.org/10.1016/j.ymben.2018.05.006.

29. Coman, V., Gustavsson, T., Finkelsteinas, A., von Wachenfeldt, C., Hägerhäll, C., and Gorton, L. (2009). Electrical wiring of live, metabolically enhanced Bacillus subtilis cells with flexible osmium-redox polymers. J. Am. Chem. Soc. *131*, 16171–16176. https://doi.org/10.1021/ja905442a.

30. Liu, W., Liu, C., and Jiang, J. (2014). [Research progress on biofilm formation by Bacillus subtilis- a review]. Weishengwu Xuebao *54*, 977–983.

31. Pankratova, G., Hederstedt, L., and Gorton, L. (2019). Extracellular electron transfer features of Gram-positive bacteria. Anal. Chim. Acta *1076*, 32–47. https://doi.org/10.1016/j.aca.2019.05.007.

32. Goyal, A., and Singhal, S. (2016). Robust and economic reduction protocol employing immensely stable and leach-proof magnetically separable nanocomposites. RSC Adv. *6*, 91275–91294. https://doi.org/10.1039/c6ra17387j.

33. Pershin, S.M., Vodchits, A.I., Khodasevich, I.A., Grishin, M.Y., Lednev, V.N., Orlovich, V.A., and Chizhov, P.A. (2020). Picosecond stimulated Raman scattering at 3000 and 3430 cm(-1) OH vibrations without optical breakdown. Opt. Lett. *45*, 5624–5627. https://doi.org/10.1364/OL.402358.

34. Dubois, V., Umari, P., and Pasquarello, A. (2004). Dielectric susceptibility of dipolar molecular liquids by ab initio molecular dynamics: application to liquid HCl. Chem. Phys. Lett. *390*, 193–198. https://doi.org/10.1016/j.cplett.2004.04.021.

35. Niki, K., Hardy, W.R., Hill, M.G., Li, H., Sprinkle, J.R., Margoliash, E., Fujita, K., Tanimura, R., Nakamura, N., Ohno, H., et al. (2003). Coupling to lysine-13 promotes electron tunneling through carboxylate-terminated alkanethiol self-assembled monolayers to cytochrome c. J. Phys. Chem. B *107*, 9947–9949. https://doi.org/10.1021/jp035392l.

36. Sawicka, A., Skurski, P., Hudgins, R.R., and Simons, J. (2003). Model calculations relevant to disulfide bond cleavage via electron capture influenced by positively charged groups. J. Phys. Chem. B *107*, 13505–13511.

37. Okamoto, A., Tokunou, Y., Kalathil, S., and Hashimoto, K. (2017). Proton transport in the outer-membrane flavocytochrome complex limits the rate of extracellular electron transport. Angew Chem. Int. Ed. Engl. *56*, 9082–9086. https://doi.org/10.1002/anie.201704241.

38. Enevoldsen, G.H., Glatzel, T., Christensen, M.C., Lauritsen, J.V., and Besenbacher, F. (2008). Atomic scale Kelvin probe force microscopy studies of the surface potential variations on the TiO2(110) surface. Phys. Rev. Lett. *100*, 236104. https://doi.org/10.1103/PhysRevLett.100.236104.

39. Cohen, G., Halpern, E., Nanayakkara, S.U., Luther, J.M., Held, C., Bennewitz, R., Boag, A., and Rosenwaks, Y. (2013). Reconstruction of surface potential from Kelvin probe force microscopy images. Nanotechnology *24*, 295702. https://doi.org/10.1088/0957-4484/24/29/295702.

40. Barth, C., and Henry, C.R. (2009). Kelvin probe force microscopy on MgO(001) surfaces and supported Pd nanoclusters. J. Phys. Chem. C *113*, 247–253. https://doi.org/10.1021/jp807340k.

41. Jakas, A., Vlahoviček-Kahlina, K., Ljolić-Bilić, V., Horvat, L., and Kosalec, I. (2020). Design and synthesis of novel antimicrobial peptide scaffolds. Bioorg. Chem. *103*, 104178. https://doi.org/10.1016/j.bioorg.2020.104178.

42. Willing, S.E., Candela, T., Shaw, H.A., Seager, Z., Mesnage, S., Fagan, R.P., and Fairweather, N.F. (2015). Clostridium difficile surface proteins are anchored to the cell wall using CWB2 motifs that recognise the anionic polymer PSII. Mol. Microbiol. *96*, 596–608. https://doi.org/10.1111/mmi.12958.

43. Schaich, K.M., and Rebello, C.A. (1999). Extrusion chemistry of wheat flour proteins: I. Free radical formation. Cereal Chemistry J. *76*, 748–755.

44. Labanowska, M., Kurdziel, M., Filek, M., Walas, S., Tobiasz, A., and Wesełucha-Birczyńska, A. (2014). The influence of the starch component on thermal radical generation in flours. Carbohydr. Polym. *101*, 846–856. https://doi.org/10.1016/j.carbpol.2013.10.005.

45. Duan, B., Yang, J., Salvador, J.R., He, Y., Zhao, B., Wang, S., Wei, P., Ohuchi, F.S., Zhang, W., Hermann, R.P., et al. (2016). Electronegative guests in CoSb3. Energy Environ. Sci. *9*, 2090–2098.

46. Lovley, D.R. (2012). Electromicrobiology. Annu. Rev. Microbiol. *66*, 391–409. https://doi.org/10.1146/annurev-micro-092611-150104.

47. Yang, H.L., Sun, Y.Z., Hu, X., Ye, J.D., Lu, K.L., Hu, L.H., and Zhang, J.J. (2019). Bacillus pumilus SE5 originated PG and LTA tuned the intestinal TLRs/MyD88 signaling and microbiota in grouper (Epinephelus coioides). Fish Shellfish Immunol. *88*, 266–271. https://doi.org/10.1016/j.fsi.2019.03.005.

48. O'Brien, J.P., and Malvankar, N.S. (2016). A simple and low-cost procedure for growing geobacter sulfurreducens cell cultures and biofilms in bioelectrochemical systems. Curr. Protoc. Microbiol. *43*, A.4K.1–A.4K.27. https://doi.org/10.1002/cpmc.20.

49. Amft, J., Steffen-Heins, A., and Schwarz, K. (2020). Analysis of radical formation by EPR in complex starch-protein-lipid model systems and corn extrudates. Food Chem. *331*, 127314. https://doi.org/10.1016/j.foodchem.2020.127314.

STAR★METHODS

KEY RESOURCES TABLE

REAGENT or RESOURCE	SOURCE	IDENTIFIER
Bacterial and virus strains		
Bacillus subtilis	Bibio. Co.	BNCC 109047
Chemicals, peptides, and recombinant proteins		
LEU Tri-peptide	Aladdin. Co.	Lot #: 11525094

RESOURCE AVAILABILITY

Lead contact

Further information and requests for resources and reagents should be directed to and will be fulfilled by the lead contact, Yaobin Zhang (zhangyb@dlut.edu.cn).

Materials availability

This study did not generate new unique reagents.

Data and code availability

Adjective data reported in this paper will be shared by the lead contact upon request. No original code was used in this study. Any additional information required to reanalyse the data reported in this paper is available from the lead contact upon request.

EXPERIMENTAL MODEL AND SUBJECT DETAILS

B. subtilis strains and LEU Tri-peptide

B. subtilis BNCC 109047 strain used in this study was purchased from Bibio. Co. *B. subtilis* cells were initially grown for activation in an LB broth medium at 25°C and spectrophotometrically measured by optical density at a wavelength of 600 nm (OD 600). When getting into the mid-exponential growth phase, the activated bacteria were transferred to BES reactors as the sole anodic inoculum for domestication. The LEU Tri-peptide (Lot #:11525094) was purchased from Aladdin. Co.

METHOD DETAILS

Extraction of cell walls

After activation, cells of *B. subtilis* solution were collected.[47] The bacteria solutions were firstly centrifuged at 2100 g/rcf and dispersed in 0.02 mol/L PBS solution (pH = 7.4, OD600 = 0.5) with 1 mmol/L phenylmethylsulfonyl fluoride (PMSF). Then the solutions were ultrasonicated for 20 min (operation for 5 s and pause for 10 s) in an ice-water bath and centrifuged at 2100 g/rcf. The collected supernatant was centrifuged at 17,000 g/rcf for 10 min and lyophilized eventually.

Bio-electro-chemical system (BES) setup

Three groups (in triplicate) of H-type microbial electrolysis cells (MEC) each with 250 mL working volume (Φ7.0 cm × 19 cm) were used in this study, and a constant potential (0.3 V versus Ag/AgCl)[48] at the anode of MEC was supplied by an electro-working station (Chenghua, CH1030C) (Figure S5A). In each MEC reactor, two carbon brushes (Φ 3.0 cm × 3.0 cm) and an Ag/AgCl electrode were used as the working, counter, and reference electrodes, respectively. The constitution of anode electrolyte (synthetic glucose-based wastewater) and cathode electrolyte are shown in Tables S1–S4. Oxygen was continuously aerated into the cathode electrolyte to serve as the terminal electron acceptor of BES during the operation, while the anode chambers were operated under anaerobic or aerobic conditions through shifting the aeration of CO_2/N_2 (20%:80%) or oxygen.

Of the three groups of MECs (Figure S5A and Table S5), the MECs without glucose (no electron donator) added were used as the background group.[10] The MECs imposed with an electric potential (0.3 V vs. Ag/AgCl) in the anode were used as the pre-electrical-domestication group. The MEC without potential but with oxygen aerated in the anode were used as the control group. In this study, all the incubation and tests were conducted at 25°C except as otherwise noted.

Electron acceptor switching test

After 9 days of cultivation, the bacteria solution in the pre-electrical-domestication group and control group were taken out to be centrifuged at 2100 g/rcf for 10 min, and then the precipitate was resuspended to the same bacteria concentration (OD_{600} = 0.8). Notably, the viability of bacteria in the pre-electrical-domestication group and control group were similar (Figure S6). The redispersed bacteria solution was added to new MEC reactors, of which the conditions were similar to the MEC reactors of the pre-electrical-domestication group. After the electric current became stable, the anodic aeration was shifted from CO_2/N_2 (20%:80%) to O_2 and then back to CO_2/N_2 to observe the current changes.

Cell walls and tripeptide treatment batches

The extracted cell walls solution and Leu tripeptide solution (0.05 mg/L, Aladdin) in triplicate, were treated in single-chamber MECs for 10 days. After aerated with 20% CO_2 balanced in N_2 for 30 min, the solution was examined with chronoamperometry in a single-chamber MEC (working volume: 100 mL), in which the carbon brush (Φ 3.0 cm × 3.0 cm) electrode, an Ag/AgCl electrode and Pt electrode (Φ 0.1 cm × 3.7 cm) were used as the working, reference and counter electrode, respectively. The MEC reactors were operated with and without a potential, respectively. And the reactors with 0.3 V (vs. Ag/AgCl) potential were used as the potential-treated group for cell walls and tripeptide, while the reactors without potential were used as the potential-free group for cell walls and tripeptide.

Detection of riboflavins

To investigate the effect of potential on the secretion of riboflavin (electron shuttle) in *B. subtilis*, the concentration of riboflavin in the effluent of the anodic electrolyte of the pre-electrical-domestication group and MFC group was measured, as the electrodes were used as terminal electron receptors for the extracellular respiration of *B. subtilis* in these two groups. The procedure for riboflavin detection was as follows: The electrolyte was firstly centrifuged at 12,000 rpm and then filtered through a 0.45 μm cellulose acetate membrane. And the supernatant was retained as samples for high-performance liquid chromatography (Agilent 1100, USA) analysis. In this test, the C18 column was used as the chromatographic column, and 30% methanol and 70% ammonium acetate (5 mM) were used as the mobile phase. The flow rate was 1 mL/min, and the column temperature was maintained at 30 °C. The detector was an FID fluorescence detector with an excitation wavelength of 450 nm and an emission wavelength of 520 nm.

Detection of respiratory enzymes

After treatment, the bacterial solution of the pre-electrical-domestication group and aerobic group were collected in triplicate. The bacterial solutions were centrifuged at 2100 g/rcf and dispersed in 0.02 mol/L PBS solution with 1 mmol/L PMSF added (pH = 7.4, OD = 0.8). Then the solutions were ultrasonicated for 20 min (operation for 5 s and pause for 10 s) in an ice-water bath. The concentrations of the respiratory enzymes in the collected solution were detected with the ELISA kits, respectively.

Optical detection

Confocal laser scanning microscopy (CLSM) (Fluoview FV-1000, Olympus, Germany) was employed to visualize the percentages of total (stained with DAPI) and dead (stained with PI) bacteria cells that were collected from the MEC reactors.

Electrochemical measurements

Cyclic voltammetry (CV) was performed with a workstation (CHI 660, Chenhua Instrument, China) in the range of −0.6 to −0.4 V at scan rates of 5 mV/s, respectively. Before the analysis, the electrolyte (20 mL tripeptide solution) in the same concentration was aerated for 15 min with N_2 to maintain the anaerobic condition. The conductivity test of cell wall solution was conducted with a conductivity meter (Mettler Toledo S230K, Switzerland).

In situ electrochemical test

The vibrational transition behaviors of the outermost surface of the cell surface during electrochemical reactions were characterized by electrochemical *in situ* Fourier transform infrared spectroscopy (FTIR, Bruker VERTEX 70). A Pt electrode (Φ 2.0 cm), Ag/AgCl electrode, and Pt sheet (15 × 15 × 0.1 mm) was used as the working, reference, and counter electrode, respectively. A thin layer configuration equipped with a CaF_2 window was placed out of the infrared spectroscopy chamber in a vertical configuration. Cells in the same concentration were firstly scattered in 2 mL Nafion solution, and then a 200 μL mixture was coated on the surface of the working electrode. Then, the electrodes were placed inside the infrared cell that was filled with ^2H_2O to avoid the dosage effect on the spectra. A workstation (CHI 660, Chenhua Instrument, China) was used to control the potential of the working electrode shifting at a range of −0.9 V–0.4 V. The wavenumber range of FTIR spectra was 500–4500 cm^{-1} and the spectra were subsequently analyzed with the OMNIC 8.0 software (Thermo Nicolet).

Kinetic isotope effect (KIE) test

To examine the KIE on current production, bacteria solution from the anode of MEC was centrifuged at 2100 g/rcf and redispersed to the same OD 600 level. Then 40 μL bacteria solution (for the KIE test of bacteria cell) or cell wall solution (for the KIE test of the cell walls) was coated on a glassy carbon electrode (Φ 0.5 cm) and dried at room temperature. The potential of the working electrode was 0.3 V (vs. Ag/AgCl), the same as the potential used in the mentioned-above experiment. The MEC reactors used here were the same as the tripeptide treatment batches except for the working electrode. After all of the I-t curves became stable, ^2H_2O was added at a final concentration of 2.0% (v/v) to observe the possible kinetic isotope effect on the electron transfer coupled with proton motion.[37] Particularly, during the operation for bacteria cells, a glucose-based electrolyte was continuously to keep bacteria active, while for cell walls, 1.0 mM PBS was used as the electrolyte.

Atomic force microscope (AFM) test

AFM topographies were obtained using the tapping mode of Asylum Research Cypher VRS AFM for the AFM test and the AM-KPFM mode of Bruker Dimension Icon AFM for the Kelvin probe force microscopy (KPFM) test with a scanning rate of 1 Hz in air. AD-2.8-AS probe and SCM-PIT probe were used for AFM and KPFM tests, respectively. The dispersed samples were applied to the nonconducting glass and dried at room temperature. A lift height of 80 nm was applied in the KPFM test. To prevent sample degradation in air, all measurements were performed within 0.5 h after samples were taken out from the nitrogen environment.

Electron paramagnetic resonance spectroscopy

The Electron paramagnetic resonance spectroscopy (EPR) measurements were performed on a Bruker Elexsys II E500-CW-EPR spectrometer (Rheinstetten, Germany) operating with an X-band at 9.85 GHz and a modulation frequency of 100 kHz at room temperature. The evaluation was performed with the Bruker-software Xepr 2.6b.52. For measurements,[49] PBN solution was prepared in a 200 mM concentration with ethanol, and then added into the potential-treated peptide solution and the control peptide solution for 1 h of electrolysis with 0.3 V versus Ag/AgCl potential applied. The EPR settings for measurement of short-lived lipid radicals were as follows: microwave attenuation = 10 dB; modulation amplitude = 1.0 G; receiver gain = 80 dB; sweep width = 100 G; microwave power = 20 mW; time constant = 163.84 ms; conversion time = 100.05 ms and center field = 3511.45 G.

X-Ray photoelectron spectroscopy (XPS)

The chemical states of Carbon (C), Oxygen (O), and Nitrogen (N) elements on the tripeptide were investigated by X-ray photoelectron spectroscopy. The element compositions were characterized by XPS got from a VG ESCALAB 250 spectrometer using a non-mono-chromatized Al Ka X-ray source (1486.6 eV) with the pass energy high-resolution scan at 30 eV and survey scan at 100 eV. Spectra were analyzed with XPSPEAK41 software (Raymond Kwok). The C 1s at 284.5 eV was used as the reference for charge correction.

QUANTIFICATION AND STATISTICAL ANALYSIS

All data are expressed as mean ± SD, and n represents the number of independent replicates or sampled values per group, as detailed in the description.